Chin. J. Astron. Astrophys. Vol. 4 (2004), No. 6, 527–532
(http://www.chjaa.org or http://chjaa.bao.ac.cn)

Chinese Journal of Astronomy and Astrophysics

A Peculiar Broad Line Radio Galaxy 1938–155: VLA Observation at 90 cm *

Tao An[1,2], Xiao-Yu Hong[1,2], Wen-Xia Feng[1,2] and Jun-Hui Zhao[3]

[1] Shanghai Astronomical Observatory, Chinese Academy of Sciences, Shanghai 200030; antao@center.shao.ac.cn
[2] National Astronomical Observatories, Chinese Academy of Sciences, Beijing 100012
[3] Harvard-Smithsonian Center for Astrophysics, 60 Garden Street, MS 78, Cambridge, MA 02138

Received 2004 March 18; accepted 2004 May 12

Abstract We observed 1938–155, a broad line radio galaxy (BLRG), with the Very Large Array (VLA) at 90 cm with an angular resolution of $6.8'' \times 4.0''$. The source consists of two components separated by 4 arcsec (~ 20 kpc, for $H_0 = 65$ km s^{-1} Mpc^{-1}, $q_0 = 0.5$) along the SE–NW direction. Both components show steep-spectra with a similar spectral index $\alpha \sim 0.83 \pm 0.07$ ($S_\nu \propto \nu^{-\alpha}$). The bright double components are surrounded by a low-brightness cocoon. The radio properties of the two bright components are consistent with the hot spots produced by twin jets. An upper limit of ~ 0.0008 for the core dominance parameter (R) is inferred, suggesting there is no prominent radio core in the source. Assuming a modest viewing angle 30°, a jet velocity is estimated $\sim 0.07\,c$, based on the jet to counter-jet brightness ratio (J). The lower limit in jet speed inferred is consistent with no Doppler beaming effect on the jet. The radio galaxy 1938–155 could be an exceptional BLRG with no prominent radio core or jet.

Key words: Galaxy: quasar: individual — radio continuum: VLA

1 INTRODUCTION

Observational studies of powerful radio galaxies are important in understanding the physics processes in extragalactic radio sources. The classical model of active galactic nuclei (AGNs) suggests that the outer extended emission is produced by a central engine at the galactic nucleus. In the framework of the 'unified schemes', the observations of AGNs are biased by the orientation of the jets with respect to the observer because of the Doppler beaming effect. The relativistic effect and jet orientation appear to play an important role in the determination of physical properties of powerful radio galaxies and quasars (Barthel 1989). Statistical studies (Morganti et al. 1997) suggested that the double-lobe Fanaroff-Riley type II (Fanaroff & Riley 1974) radio

* Supported by the National Natural Science Foundation of China.

galaxies are subject to a stronger beaming effect than the FR I objects. Furthermore, among the FR II radio galaxies the jets in the observed BLRGs (Broad Line Radio Galaxies) appear to prefer to be aligned with the line of sight, and it is generally expected that the BLRGs will show a stronger Doppler beaming effect. Hardcastle et al. (1998) also suggested that high-luminosity BLRGs are preferentially aligned to the line of sight in comparison with the NLRGs (Narrow Line Radio Galaxies). The radio cores and kiloparsec-scale jets in FR II BLRGs are prominent against the surrounding extended emission. However, in some of BLRGs, we have not observed any significant radio core with jet structure. The radio galaxy 1938–155 appears to one exceptional BLRG in this regard.

The radio galaxy 1938–155 (also named OV 164) was identified as a BLRG with $m_V = 21.5$ mag. Its redshift was estimated to be 0.452 from the emission line (Tadhunter et al. 1993; Dickson et al. 1997). At the distance of 1938–155, 1 arcsec corresponds to ~ 5 kpc ($H_0 = 65$ km s^{-1} Mpc^{-1}, $q_0 = 0.5$). The low-resolution VLA C-array image at 6 cm showed a cocoon-like structure with two clear peaks along the SE-NW direction (Morganti et al. 1993). In the high-resolution radio images of 1938–155 obtained by the VLA A-array and Australia Telescope Compact Array (ATCA), two bright lobes dominated the total intensity (Morganti et al. 1999). The eastern lobe was much brighter than the western one, and showed a stronger depolarization between 6 cm and 3 cm. The low-brightness cocoon was fully resolved. There was no distinct core or jet between the two lobes. The source exhibits a steep spectrum at radio wavelengths from 80 MHz to 31.4 GHz (`http://nedwww.ipac.caltech.edu`). The source was described as an FR II radio galaxy for its high radio power and double-lobe radio morphology (Tadhunter et al. 2002).

In this paper, we present results from observations of 1938–155 at 90 cm with the VLA. The physical properties and non-detection of core at the lower radio frequency will also be discussed.

2 OBSERVATION AND DATA REDUCTION

The radio galaxy 1938–155 was observed with the VLA in its A array configuration on June 17, 2003. The source was used as a calibrator in a VLA program for low-frequency observations of the Galactic center. The observations were performed in special line mode in order to reject radio frequency interference (RFI) and minimize the bandwidth smearing effect at low frequencies. The correlator was set with two IFs (centered at 303 MHz and 330 MHz), each 3.125 MHz bandwidth.

The quasar 3C 48 was observed at the end of the observations and used to determine the scale of flux density. We observed 1938–155 for nine scans with a total integral time about 22 minutes in the entire observation track of 8 h. The data were calibrated and corrected for errors in both phase and amplitude using the Astronomical Image Processing System (AIPS) of the National Radio Astronomy Observatory (NRAO). Further process in the data reduction including editing, self-calibration in both amplitude and phase, and imaging was carried out using both the AIPS and DIFMAP packages (Shepherd, Pearson & Taylor 1994). The uncertainty in flux density is $\sim 5\%$ due to errors in the gain calibration.

Table 1 VLA Observation at 90 cm and the Image Parameters

Figure	Conf.	Resolution (P.A.) arcsec (°)	$S_{\rm peak}$ Jy beam^{-1}	rms mJy beam^{-1}	$S_{\rm tot}$ Jy
Figure 1*	VLA-A	6.8×4.0 (15)	11	6.7	20.0

*: super-resolved image, ROBUST= −2, UVBOX= 3 are used in task IMAGR.

3 RESULTS AND DISCUSSION

Figure 1 shows an image of 1938–155 observed at 90 cm with the VLA. The image was made with uniform weight (a restored beam of $6.8'' \times 4.0''$). The image parameters are summarized in columns 4–6 of Table 1. The total intensity of the source is determined by integrating the source in the final CLEANed image. The dynamic range of the image is ∼1700:1 in Fig. 1.

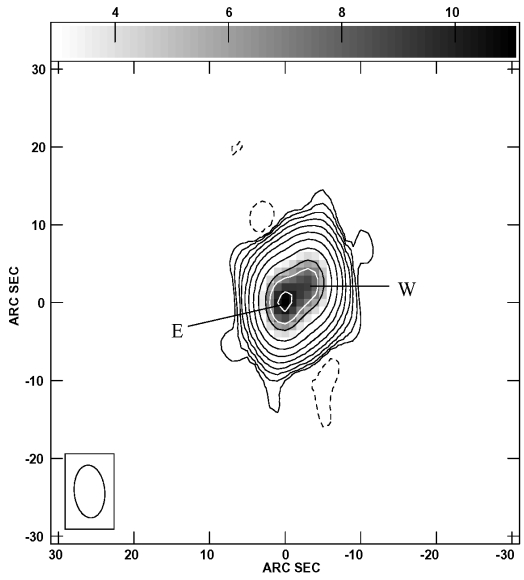

Fig. 1 Total intensity image of 1938–155. The grey scale ranges between 3 and 11 Jy beam^{-1}. The restored beam is $6.8'' \times 4.0''$ (PA=15°). The peak flux density is 11.2 Jy beam^{-1}. The contours are 0.02× (−1, 1, 2, 4, 8, 16, 32, 64, 128, 256, 384, 512) Jy beam^{-1}.

Table 2 Parameters of the Gaussian Components

Comp.	$S_{\rm peak}$ (Jy b^{-1})	$S_{\rm int}$ (Jy)	r (arcsec)	θ (°)	Maj (arcsec)	Min (arcsec)	ϕ (°)
E	10.9 ± 0.5	11.5 ± 0.23	0.36 ± 0.02	94.4 ± 7.4	1.84 ± 0.09	0.46 ± 0.17	126 ± 1.9
W	8.0 ± 0.4	8.50 ± 0.17	4.31 ± 0.10	-52.7 ± 9.2	1.54 ± 0.03	0.87 ± 0.01	129 ± 0.2

It has been known that 1938–155 consists of two components, marginally resolved in the VLA observation (Fig. 1). The 90 cm image shows that the source is elongated in the SE–NW direction. This result is consistent with the VLA observations at 6 cm in the C-configuration with a resolution of $6.1'' \times 3.0''$ (Morganti et al. 1993). A bright peak is detected near the phase center of the synthesized image. A secondary peak is observed northwest to the primary peak, separated by $\sim 4''$. To quantitatively study the radio structure, we carried out a model fitting to the data. The task MODELFIT in the DIFMAP package and task JMFIT in AIPS were

used to fit the VLA data. Two Gaussians, E and W, respectively in Fig. 1 appear to fit the data very well. Table 2 summarizes the parameters of the Gaussian components. Here $S_{\rm peak}$ and $S_{\rm int}$ correspond to the peak flux density and the integral flux density, respectively; r and θ are the radial separation and the position angle of the component with respect to the phase center; Maj and Min are the sizes along the major and minor axes of each of the Gaussian components; ϕ is the position angle of the major axis. The errors in flux density of the model components contain both uncertainties in the calibration and model fitting. The error in position of each component is dominated by the difference in fit position between the two procedures JMFIT and MODELFIT.

The integrated flux density of the component E is greater than that of W by about 3 Jy. The sum of the flux densities in both components contains 99% of the total flux density of the entire source observed with the VLA in the A-configuration. Figure 2 shows the radio intensity distribution along P.A. 127° (or P.A.−53°). The E and W components (dashed line) with an angular separation of 4″ are clearly suggested in Fig. 1.

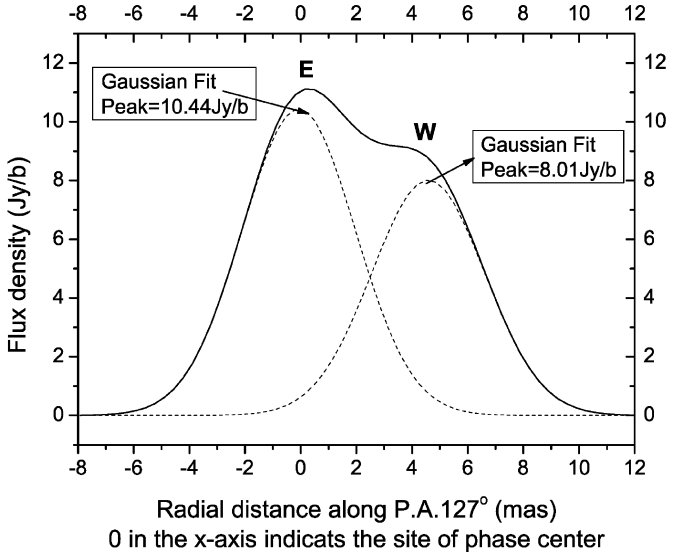

Fig. 2 Flux density distribution along P.A. 127° (the solid line). Two dash lines mark the two Gaussian components fitted to the slice corresponding to the components E and W.

We note that the low resolution observations of 1938–155 are good for detecting extended emission, while the high resolution observations (Morganti et al. 1999) may reveal the detailed structure of the lobes or hot spots. The components E and W actually correspond to the two lobes found by Morganti et al. (1999). Combining the flux densities of components E and W (Table 2) with the measurements at 4.8 and 8.6 GHz published in Mortanti et al. (1999), we found that the overall spectra of both components can be fit with a power law with a spectral index of $\alpha = 0.83 \pm 0.07$ ($S_\nu \propto \nu^{-\alpha}$) in E and W. Figure 3 shows that a power-law spectrum ($S_\nu \propto \nu^{-0.83}$) is well fitted with the data points. The steep spectra of both components are consistent with an optically thin, synchrotron emission, and these are consistent with the hypothesis that both E and W are lobes or hot spots of jets rather than a compact radio core.

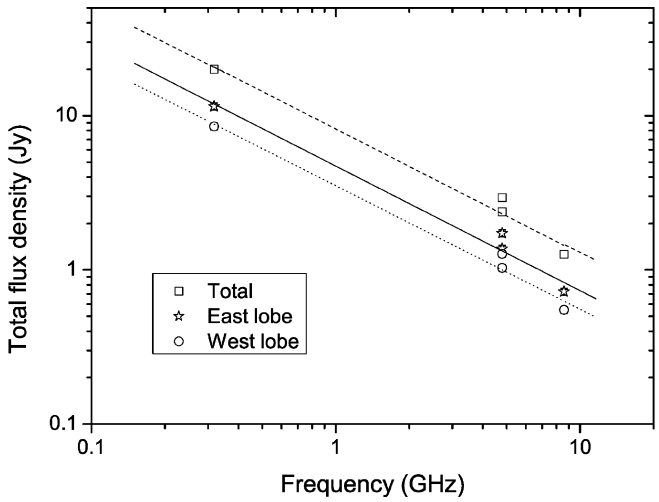

Fig. 3 A power law, $S_\nu \propto \nu^{-0.83}$, fits well the data points. The data points used in the plot: 318 MHz (the present paper); 4.8 GHz and 8.6 GHz (Morganti et al. 1999). *Square*, *Star* and *Circle* represent the measured flux of the whole source, the east lobe and the west lobe, respectively.

A typical FR II radio galaxy usually shows a prominent radio core with double bright lobes on each side. In some cases, a straight one-sided jet is observed to link a radio lobe to the nucleus (Ghisellini et al. 1993; Morganti et al. 1997; Urry et al. 1995). The observed morphologies of FR II radio galaxies appear to be subject to the Doppler beaming effect. The orientation of the radio source appears to be an important factor in the observations of the FR II radio galaxies. In the "unified schemes", BLRGs belong to aligned objects and have optical spectra dominated by broad emission lines. BLRGs usually show strong cores in their radio morphologies (Morganti et al. 1997). Broad emission lines were detected from the radio galaxy 1938–155 (Dickson et al. 1997).

These observations appear to be consistent with that the emission from the core and both the lobes in 1938–155 is aligned in the direction close to the line of sight. However, the radio images with different resolutions at different wavelengths did not detect a core or jet between the two lobes (Morganti et al. 1993, 1999 and present paper). The lack of emission from the core at 90 cm could be due to either self-absorption or free-free absorption by thermally ionized gas in the nuclear region.

To estimate the core dominance parameter ($R = S_{\rm core}/S_{\rm lobe}$) in 1938–155, a residual r.m.s. of ~ 0.015 Jy is estimated after the emission from both lobes is taken out. This should be an upper limit of the flux density in the core. Therefore an upper limit of 0.0008 is inferred for the core dominance. It is much lower than the average for BLRGs ($R \sim 0.027$, Morganti et al. 1999). This is because the optically thin synchrotron emission from the lobes greatly increases at long wavelength.

In the relativistic beaming model, the jet-to-counterjet brightness ratio (J) can be used as a beaming indicator. If we assume the brighter lobe E in 1938–155 moves towards us, and the lobe W is associated with the counter jet, then a ratio J of 1.4 is inferred. Assuming the jet and counterjet have a same intrinsic velocity, we obtain an estimate for the jet speed, $\beta\cos(\theta) \sim 0.06\,c$. Assuming a modest viewing angle of 30° for a FR II radio galaxy in the

unified scenario (Urry & Padovani 1995), we found the jet speed is about $0.07\,c$. We note that this inferred jet speed can only be used as a lower limit since the motion of the gas in the lobes is substantially decelerated by the interstellar medium.

Although the low core dominance parameter and low jet speed in 1938–155 might suggest that the radio core is not beamed toward us, the 90 cm data appear to be inadequate to exclude other possibilities such as nuclear absorption by a self-synchrotron absorption process or by a free-free absorption from the nuclear ionized gas. Alternatively, the non-detection of radio core or jet in 1938–155, an FR II BLRG, can be explained by the observations being insufficiently sensitive.

Finally, the non-detection could also be related to a special intrinsic physical condition in the source. The intrinsic core luminosity and jet efficiency might vary in radio sources. The BLRG 1938–155 could be a special case with relatively lower jet radiative efficiency.

4 SUMMARY

We present the radio image of 1938–155 at a low frequency 330 MHz, or wavelength 90 cm. Two optically thin, synchrotron components characterized by steep-spectra appear to dominate the radio source. The double components are surrounded by a low-brightness cocoon. There is no prominent radio core observed at 90 cm. The low upper limit in the core dominance and the low jet speed are consistent with no beamed emission from the core of the source. However, our data can not rule out other possibilities of explaining the absence or the non-detection of radio core and jets.

Acknowledgements This research is supported by the National Natural Science Foundation of China (10328306 and 10333020). The author is grateful for the technique support by the staff of VLA. VLA, as a facility of the National Radio Astronomy Observatory, is operated by Associated Universities Inc. under the cooperative agreement with the National Science Foundation. This research has made use of the NASA/IPAC Extragalactic Database (NED).

References

Barthel P. D., 1989, ApJ, 336, 606
Dickson R., 1997, Ph. D. Thesis, Univeristy of Sheffield
Fanaroff B. L., Riley J. M., 1974, MNRAS, 167, 31
Ghisellini G., Padovani P., Celotti A., Maraschi L., 1993, ApJ, 407, 65
Hardcastle M. J., Alexander P., Pooley G. G., Riley J. M., 1998, MNRAS, 296, 445
Hardcastle M. J., Alexander P., Pooley G. G., Riley J. M., 1999, MNRAS, 304, 135
Morganti R., Killeen N. E. B., Tadhunter C. N., 1993, MNRAS, 263, 1023
Morganti R., Oosterloo T. A., Reynolds J. E. et al., 1997, MNRAS, 284, 541
Morganti R., Oosterloo T., Tadhunter C. N. et al., 1999, A&ASS, 140, 355
Seibert J., Brinkmann W., Morganti R. et al., 1996, MNRAS, 279, 1331
Shepherd M. C., Pearson T. J., Taylor G. B., 1994, BAAS, 26, 987
Tadhunter C. N., Morganti R., di Serego Alighieri S., 1993, MNRAS, 263, 999
Tadhunter C. N., Dickson R., Morganti R. et al., 2002, MNRAS, 330, 977
Urry C. M., Padovani P., 1995, PASP, 107, 803